Research in Astron. Astrophys. **2013** Vol. **13** No. **4**, 411–419
http://www.raa-journal.org *http://www.iop.org/journals/raa*

Research in Astronomy and Astrophysics

Multi-wavelength emission from 3C 66A: clues to its redshift and gamma-ray emission location *

Da-Hai Yan, Zhong-Hui Fan, Yao Zhou and Ben-Zhong Dai

Department of Physics, Yunnan University, Kunming 650091, China; *yandahai555@gmail.com*; *fanzh@ynu.edu.cn*; *bzhdai@ynu.edu.cn*

Received 2012 August 23; accepted 2012 November 12

Abstract The quasi-simultaneous multi-wavelength emission of TeV blazar 3C 66A is studied by using a one-zone multi-component leptonic jet model. It is found that the quasi-simultaneous spectral energy distribution of 3C 66A can be well reproduced; in particular, the first three months of its average *Fermi*-LAT spectrum can be well reproduced by the synchrotron self-Compton component plus external Compton component of the broad line region (BLR). Clues to its redshift and gamma-ray emission location are obtained. The results indicate the following. (i) On the redshift: The theoretical intrinsic TeV spectra can be predicted by extrapolating the reproduced GeV spectra. Through comparing these extrapolated TeV spectra with the corrected observed TeV spectra from extragalactic background light , it is suggested that the redshift of 3C 66A could be between 0.1 and 0.3, with the most likely value being ~ 0.2. (ii) On the gamma-ray emission location: To well reproduce the GeV emission of 3C 66A under different assumptions on the BLR, the gamma-ray emission region is always required to be beyond the inner zone of the BLR. The BLR absorption effect on gamma-ray emission confirms this point.

Key words: BL Lacertae objects: individual (3C 66A) — galaxies: active — gamma-rays: theory — radiation mechanisms: non-thermal

1 INTRODUCTION

Blazars are the most extreme class of active galactic nuclei (AGNs). Their spectral energy distributions (SEDs) are characterized by two distinct bumps. The low-energy component originates in relativistic electron synchrotron emission. The high-energy component could be produced by inverse Compton (IC) scattering (e.g., Böttcher 2007). Various soft photon sources seed a synchrotron self-Compton (SSC) process (e.g., Rees 1967; Maraschi et al. 1992) and an external Compton (EC) process (e.g., Dermer & Schlickeiser 1993; Sikora et al. 1994) in the jet to produce γ-rays. Hadronic models have also been proposed to explain the multi-band emissions of blazars (e.g., Mannheim 1993; Mücke et al. 2003).

TeV photons emitted by blazars are absorbed through the pair-production process, by interaction with extragalactic background light (EBL) (Stecker et al. 1992). The absorption effect depends on both the EBL photon density and the redshift of the TeV source. The energy range of interest for

* Supported by the National Natural Science Foundation of China.

background photons here is from optical to ultraviolet (UV). Since it is difficult to measure the EBL directly, many EBL models are proposed, such as low limit models (e.g., Kneiske & Dole 2010; Razzaque et al. 2009), mean level ones (e.g., Finke et al. 2010; Franceschini et al. 2008), and high level ones (e.g., Stecker et al. 2006). Aharonian et al. (2006) discussed some gamma-ray blazars with unexpectedly hard spectra at relatively large redshift, and suggested that EBL is the first type. Albert et al. (2008) found that the universe is more transparent to gamma-rays. However, Stecker & Scully (2009) pointed out that Albert et al. (2008) do not significantly constrain the intergalactic low energy photon spectra and their high level EBL model is still valid. In an analysis of photons above 10 GeV from gamma-ray sources detected by *Fermi*-LAT, Abdo et al. (2010a) found evidence to exclude the high level EBL models. The EBL absorption effect on gamma-rays is helpful to constrain the redshift of TeV sources. For instance, the SED of a blazar can be extrapolated into the TeV region by reproducing the multi-band (optical-GeV band) data with a certain emission model. The redshift of the very high energy source can then be constrained by comparing the EBL-corrected, observed TeV spectrum with the extrapolated one.

It is well known that the high energy emissions of some blazars need EC components (e.g., Gao et al. 2011). The energy density of the external photon field is related to the gamma-ray emission location (e.g., Ghisellini & Tavecchio 2009). Therefore, the clue to the gamma-ray emission region location in a blazar can be obtained from its high energy emission (e.g., Yan et al. 2012). Moreover, the external photon absorption of the gamma-ray emission is also helpful to constrain the gamma-ray emission location of a blazar (e.g., Liu et al. 2008; Bai et al. 2009; Poutanen & Stern 2010).

3C 66A is classified as an intermediate BL Lac (IBL), because its synchrotron emission peaks between 10^{14} Hz and 10^{15} Hz (Perri et al. 2003; Abdo et al. 2010b). The most widely used redshift for 3C 66A is 0.444, based on a single emission line measurement (Miller et al. 1978). However, Miller et al. (1978) stated that they were not sure of the reality of this emission feature, and warned that the redshift is not reliable. Later, Lanzetta et al. (1993) confirmed the redshift of 0.444 based on data from the *International Ultraviolet Explorer* (*IUE*). However, Bramel et al. (2005) argued that the 3C 66A redshift determined using *IUE* data is questionable. Finke et al. (2008) placed a lower limit on the redshift of 3C 66A, $z \geq 0.096$, using information regarding its host galaxy. Recently, Prandini et al. (2010) suggested that the redshift of 3C 66A should be below 0.34 ± 0.05, and that the most likely redshift is 0.21 ± 0.05, by assuming that the EBL-corrected TeV spectrum is not harder than the *Fermi*-LAT spectrum.

Joshi & Böttcher (2007) suggested that γ-ray emission of 3C 66A in the flare state could be dominated by an EC process. Yang & Wang (2010) found that the TeV emission has a contribution from EC when taking $z = 0.444$, or by pure SSC when $z = 0.1$. Abdo et al. (2011) studied the SED of 3C 66A at flare state by using the SSC+EC model, and suggested that the redshift of 3C 66A could be between 0.2 and 0.3.

A campaign of quasi-simultaneous multi-wavelength observations for 3C 66A was carried out by *Fermi* and *Swift* from 2008 August to 2008 October. VERITAS observed 3C 66A for 14 hours from 2007 September through 2008 January and for 46 hours between 2008 September and 2008 November (Acciari et al. 2009, 2010). In this work, the first three month average spectrum from *Fermi*-LAT and the average spectrum from VERITAS based on the observations from 2007 September through 2008 November are used. Data from the radio, optical, UV, X-ray, and GeV γ-ray to TeV γ-ray bands are publicly available (Abdo et al. 2010b). In this work, we study the quasi-simultaneous SED of 3C 66A with a multi-component leptonic jet model, and constrain its redshift and gamma-ray emission location. We adopt the cosmological parameters $(H_0, \Omega_m, \Omega_\Lambda)$ = (70 km s^{-1} Mpc^{-1}, 0.3, 0.7) throughout this paper.

2 THE MODEL

We assume that multi-band emission of a blazar is produced in a spherical blob in the jet, which is moving relativistically at a small angle with respect to our line of sight. The observed radiation is

strongly boosted by a relativistic Doppler factor $\delta_{\rm D}$. The relativistic electrons inside the blob lose energy via synchrotron emission and IC scattering. The electron distribution is (Dermer et al. 2009)

$$\begin{aligned} N'_{\rm e}(\gamma') = \; & K'_{\rm e} H(\gamma';\gamma'_{\rm min},\gamma'_{\rm max})\gamma'^{-p_1}\exp(-\gamma'/\gamma'_{\rm b}) \times H[(p_2-p_1)\gamma'_{\rm b}-\gamma'] \\ & +[(p_2-p_1)\gamma'_{\rm b}]^{p_2-p_1}\gamma'^{-p_2}\exp(p_1-p_2) \times H[\gamma'-(p_2-p_1)\gamma'_{\rm b}] \\ & \times K'_{\rm e} H(\gamma';\gamma'_{\rm min},\gamma'_{\rm max}), \end{aligned} \tag{1}$$

where $K'_{\rm e}$ is the normalization factor, which describes the number of relativistic electrons in the emitting blob. $H(x;x_1,x_2)$ is the Heaviside function: $H(x;x_1,x_2)=1$ for $x_1 \le x \le x_2$ and $H(x;x_1,x_2)=0$ everywhere else; in addition $H(x)=0$ for $x<0$ and $H(x)=1$ for $x \ge 0$. In the co-moving frame, this distribution is a double power law with two energy cutoffs: $\gamma'_{\rm min}$ and $\gamma'_{\rm max}$. The spectrum is smoothly connected with indices p_1 and p_2 below and above the electrons' break energy $\gamma'_{\rm b}$ respectively. Note that here and throughout the paper, unprimed quantities refer to the observer's frame and primed ones refer to the co-moving frame.

The multi-component model of Dermer et al. (2009) is used to reproduce the SED of 3C 66A. For EC components, we consider photons directly emitted from the accretion disk and photons from the central source that are Thomson scattered in the broad line region (BLR) to be the seed photons. In addition, we take into account gamma-ray attenuation by the BLR-scattered radiation field.

We assume that the BLR is a spherically symmetric shell with inner radius $R_{\rm i}$ and outer radius $R_{\rm o}$. It is assumed that the gas density of the BLR has the power-law distribution $n_{\rm e}(r)=n_0(\frac{r}{R_{\rm i}})^{\zeta}$, where $R_{\rm i} \le r \le R_{\rm o}$. The radial Thomson depth is given by $\tau_{\rm T}=\sigma_{\rm T}\int_{R_{\rm i}}^{R_{\rm o}} dr n_{\rm e}(r)$, where r is the distance from the central black hole (Dermer et al. 2009). In our calculation, we use $\tau_{\rm T}=0.01$, which is a typical value (Finke & Dermer 2010; Reimer 2007; Donea & Protheroe 2003). Kaspi & Netzer (1999) suggested that the particle density of BLR scales as $r^{-1.0}$ or $r^{-1.5}$. In our calculation, we adopt the exponent $\zeta=-1.0$.

Using reverberation mapping, Bentz et al. (2009) derived an improved empirical relationship between BLR radius $R_{\rm BLR}$ and luminosity L_λ at 5100Å

$$\log(R_{\rm BLR}) = -21.3 + 0.519 \cdot \log(\lambda L_\lambda(5100\text{Å}))\,. \tag{2}$$

The V-band magnitude of 3C 66A is 15.21 (Véron-Cetty & Véron 2010). We use the optical spectral index given by Fiorucci et al. (2004) to calculate the average flux at 5100Å, which is 2.785 mJ. In this work, we take the estimated $R_{\rm BLR}$ as the outer radius of the BLR $R_{\rm o}$. Peterson et al. (1994) suggested that the typical size of the BLR in quasars is on the order of light-months. We follow several authors (Reimer 2007; Donea & Protheroe 2003) and use the relationship $R_{\rm i}=R_{\rm o}/40$ to derive a value for $R_{\rm i}$.

To simplify the calculation, the BLR-scattered photon field is assumed to be monochromatic with energy ϵ_*, which is the mean energy from the accretion disk (Dermer et al. 2009). The approximation for the mean dimensionless photon energy from a standard accretion disk (Shakura & Sunyaev 1973) at radius R is given by (e.g., Dermer et al. 2009; Finke & Dermer 2010)

$$\epsilon_{\rm d}(R) = 1.5\times10^{-4}\left(\frac{10\ell_{\rm Edd}}{M_8\eta}\right)^{\frac{1}{4}}\left(\frac{R}{r_{\rm g}}\right)^{-\frac{3}{4}}. \tag{3}$$

The accretion luminosity is $\ell_{\rm Edd}=\frac{L_{\rm d}}{L_{\rm Edd}}$, which here has the value of 0.03. The Eddington luminosity is $L_{\rm Edd}=1.26\times10^{46}M_8\,{\rm erg\ s^{-1}}$, and $L_{\rm d}$ is the accretion disk luminosity. The accretion efficiency η is 0.1. The gravitational radius $r_{\rm g}=\frac{GM}{c^2}\cong1.5\times10^{13}M_8\,{\rm cm}$, where c is the speed of light. The black hole mass of 3C 66A is $M_8=\frac{M_{\rm BH}}{10^8M_\odot}=4.0$ (Ghisellini et al. 2010). In this work, we adopt $\epsilon_*=\epsilon_{\rm d}(10r_{\rm g})=2.48\times10^{-5}$, corresponding to the energy of 13 eV, which is the typical

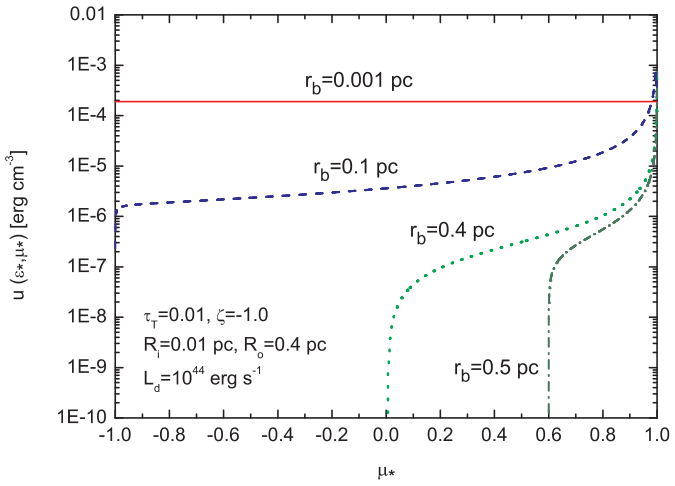

Fig. 1 Angle-dependent energy density of the BLR-scattered photon field. The values of $r_{\rm b}$ are labeled on the curves. The dimensionless photon energy is $\epsilon_* = 2.48 \times 10^{-5}$.

energy of photons from a standard accretion disk. The energy density of a BLR-scattered photon field is

$$u(\epsilon_*, \mu_*; r_{\rm b}) = \frac{L_{\rm d} r_{\rm e}^2}{3 c r_{\rm b}} F(\mu_*, r_{\rm b}) \tag{4}$$

(Dermer et al. 2009), where $r_{\rm e}$ is the classical electron radius. $r_{\rm b}$ is the distance from the emission blob to the central black hole. $F(\mu_*, r_{\rm b})$ is the function given by Dermer et al. (2009) (their eq. (97)), which is related to the gas energy density in BLR $n_{\rm e}(r_{\rm b})$. Here, $\tau_{\rm T}$ is used to normalize $n_{\rm e}(r_{\rm b})$. The energy density of the BLR-scattered photon field is angle-dependent. θ_* is the angle between the directions of the BLR scattered photon and motion of the blob, which is also the interaction angle between the relativistic electron and soft photon (Dermer et al. 2009). μ_* is the value of cosθ_*. In Figure 1, we show the energy density of the BLR-scattered photon field, varying with $r_{\rm b}$.

The intrinsic high energy photon flux from extragalactic sources is

$$f_{\rm intrinsic}(E_\gamma) = {\rm e}^{\tau(E_\gamma, z)} f_{\rm observed}(E_\gamma)\,, \tag{5}$$

where $f_{\rm observed}$ is the measured TeV flux, and $\tau(E_\gamma, z)$ is the optical depth of the γ-ray with energy E_γ at redshift z.

Here, we use the EBL model of Franceschini et al. (2008)[1] to de-absorb the observed TeV spectra. This model is based on observations and takes into account all available information on cosmic sources that are contributing background photons.

Several parameters in our model can be constrained by observations. Böttcher et al. (2009) excluded extreme values of the Doppler factor in the range $\delta_{\rm D} \geq 50$. The size of the emission blob can be constrained by the observed variability timescale $t_{\rm var}$, because $R'_{\rm b} = t_{\rm v,min} \delta_{\rm D} c/(1+z) \leq \delta_{\rm D} c t_{\rm tar}/(1+z)$. Here $R'_{\rm b}$ is the radius of the blob in the co-moving frame, and $t_{\rm v,min}$ is the smallest variability timescale. Takalo et al. (1996) reported a microvariability with $t_{\rm var} \sim 2.16 \times 10^4$ s and $\Delta{\rm mag} \sim 0.2$. Abdo et al. (2011) reported shorter variability at the optical band: $t_{\rm var} \sim 1.44 \times 10^4$ s.

[1] Opacities for photon-photon interaction as a function of the source redshift are available on the the website *http://www.astro.unipd.it/background*.

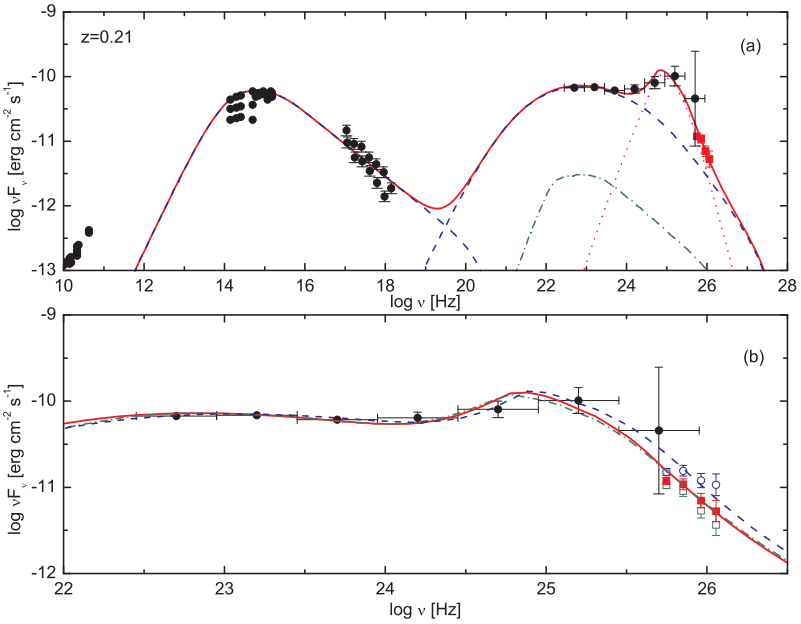

Fig. 2 In panel (a), we show the reproduced SED with $z = 0.21$. The filled squares are the de-absorbed TeV data with $z = 0.21$. The dashed, dash-dotted, dotted and thick solid lines are the SSC component, accretion-disk, BLR-reproduced component and the sum of multiple components, respectively. In panel (b), the open squares, filled squares and open circles are the de-absorbed TeV data with $z = 0.15$, 0.21 and 0.31, respectively. The dash-dotted, solid and dashed lines are the model results at $z = 0.15$, 0.21 and 0.31, respectively. The filled circles are quasi-simultaneous data from radio to GeV. All observed data are from Abdo et al. (2010b). See detailed information about the data in Abdo et al. (2010b).

3 THE RESULTS

In Figure 2, we show the modeling results at three different redshifts. The filled circles are quasi-simultaneous data from radio to GeV. The observed VERITAS data are EBL-corrected by using the EBL model of Franceschini et al. (2008) with different redshifts. It can be seen that the accretion-disk component is negligible compared to the SSC and BLR components. SSC and EC are responsible for emissions at the GeV-TeV bands. Emission between 0.1 GeV and 10 GeV is dominated by SSC. Above 10 GeV, the EC component of BLR is more important. Table 1 lists all model parameters.

It is interesting that the Klein-Nishina (KN) effect becomes important in Compton scattering the BLR radiation when $\gamma'\Gamma_{\rm bulk}\epsilon_* \geq 1/4$, where $\Gamma_{\rm bulk}$ is the bulk Lorentz factor of the blob. In our model, $\Gamma_{\rm bulk} \approx \delta_{\rm D}$, so that $\gamma'_{\rm KN} = 280$. Electrons with this energy scatter photons primarily to energy of $\epsilon_{\rm KN} \approx \Gamma_{\rm bulk}\delta_{\rm D}\epsilon_*\gamma'^2_{\rm KN}/(1+z) \approx 2.08 \times 10^3$, which corresponds to a frequency of $\nu_{\rm KN} \approx 2.57 \times 10^{23}$ Hz. Due to the KN effect, spectra from the BLR-component at the right side of the peak decline more quickly. In addition to large $\gamma'_{\rm min}$, the KN effect is the other cause of the narrow BLR-component SED.

As shown in panel (b) of Figure 2, the EBL-corrected TeV spectrum is steeper than the extrapolated one if the redshift is below 0.15. On the other hand, if the redshift is above 0.31, the EBL-corrected TeV spectrum becomes harder. The EBL-corrected TeV emission can be well reproduced when $z = 0.21$. Hence, the redshift of 3C 66A should be between 0.15 and 0.31, and the most likely

Table 1 Model Parameters for Fig. 2

Parameters	$z = 0.15$	$z = 0.21$	$z = 0.31$
B (G)	0.168	0.168	0.168
$K'_{\rm e}$ (10^{53})	0.62	1.5	1.5
p_1	2.0	2.0	2.0
p_2	4.0	4.0	4.0
$\gamma'_{\rm max}$ (10^6)	3.0	3.0	3.0
$\gamma'_{\rm b}$ (10^3)	5.8	6.3	7.6
$\gamma'_{\rm min}$ (10^3)	1.93	1.90	1.76
$\delta_{\rm D}$	38	36	43
$t_{\rm v,min}$ (10^4s)	0.69	1.17	1.21
M_8	4.0	4.0	4.0
$\ell_{\rm Edd}$	0.03	0.03	0.03
η	0.1	0.1	0.1
$\tau_{\rm T}$	0.01	0.01	0.01
ζ	–1.0	–1.0	–1.0
$R_{\rm i}$ (10^{-2}pc)	0.25	0.35	0.55
$R_{\rm o}$ (pc)	0.1	0.14	0.22
$r_{\rm b}$ ($R_{\rm o}$)	1.03	0.89	0.72

Table 2 Model Parameters for Fig. 3

Parameters	$\ell_{\rm Edd} = 0.01$	$\frac{R_{\rm o}}{R_{\rm i}} = 5$	$\tau_T = 0.1$	$\zeta = -2$
B (G)	0.168	0.168	0.168	0.168
$K'_{\rm e}$ (10^{53})	1.5	1.5	1.6	1.5
p_1	2.0	2.0	2.0	2.0
p_2	4.0	4.0	4.0	4.0
$\gamma'_{\rm max}$(10^6)	3.0	3.0	3.0	3.0
$\gamma'_{\rm b}$(10^3)	6.3	6.3	5.6	6.3
$\gamma'_{\rm min}$(10^3)	1.8	2.0	2.5	1.9
$\delta_{\rm D}$	36	36	37	36
$t_{\rm v,min}$(10^4s)	1.2	1.17	1.05	3.2
M_8	4.0	4.0	4.0	4.0
$\ell_{\rm Edd}$	–	0.03	0.03	0.03
η	0.1	0.1	0.1	0.1
$\tau_{\rm T}$	0.01	0.01	–	0.01
ζ	–1.0	–1.0	–1.0	–
$R_{\rm i}$ (10^{-2}pc)	0.35	2.8	0.35	0.35
$R_{\rm o}$ (pc)	0.14	0.14	0.14	0.14
$r_{\rm b}$ ($R_{\rm o}$)	0.65	1.02	1.31	0.52

redshift is 0.21. There are several poorly constrained parameters in our model. It should be discussed whether the uncertainties of model parameters can affect our results. As mentioned above, the contribution of the BLR component is dominant at TeV band, which is crucial for constraining the redshift of 3C 66A. The BLR structure ($R_{\rm i}$, $R_{\rm o}$, ζ, $\tau_{\rm T}$) and the characteristics of the central source (the black hole and its accretion disk) can affect the contribution of the BLR component. $R_{\rm o}$ can be constrained by Equation (2). We assumed typical values, $(\ell_{\rm Edd}, R_{\rm o}/R_{\rm i}, \tau_{\rm T}, \zeta) = (0.03, 40, 0.01, -1)$, to reproduce the SED of 3C 66A. The effects of these parameters on estimating the redshift are discussed by using other plausible boundary values. Results are shown in Figure 3(a), (b), (c) and (d). Parameters are listed in Table 2. For clarity, only the modeling results in the high energy part of the case $z = 0.21$

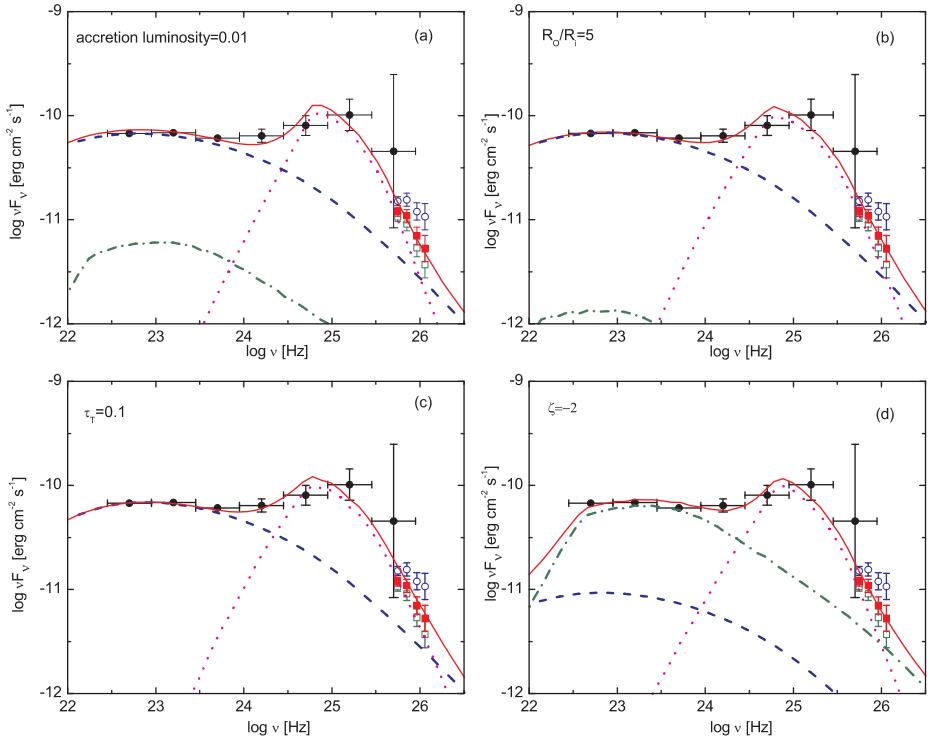

Fig. 3 The effects of different assumptions on BLR structure and the characteristics of the central source on the estimation of the redshift. The symbols are the same as those in Fig. 2.

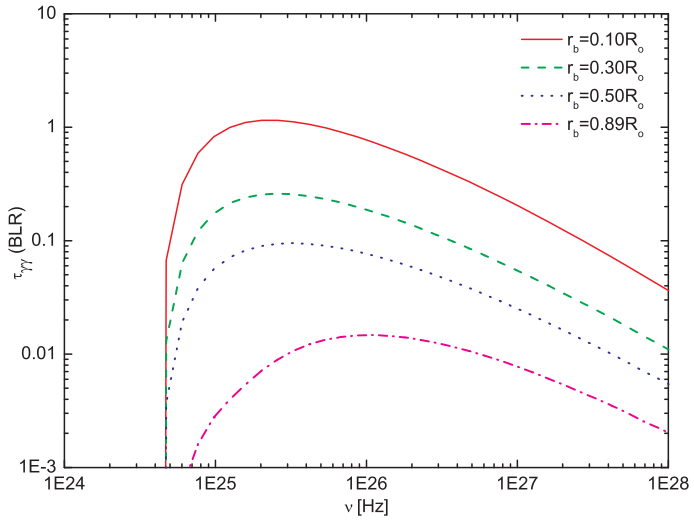

Fig. 4 $\gamma\gamma$ optical depth for γ-ray interaction with BLR-reproduced photons at different distances from the central BH when $z = 0.21$.

are shown. Obviously, the SED (including TeV spectra) can also be reproduced well. We therefore argue that our results are independent of these parameters.

In addition, our results indicate that the gamma-ray emission region is beyond the inner zone of the BLR (~ 0.1 pc, see Tables 1 and 2).

In Figure 4, we show the $\gamma\gamma$ absorption by BLR-scattered radiation at different blob locations when taking $z = 0.21$. There is a significant absorption when the blob is inside the inner zone of the BLR. Beyond the inner zone, absorption is negligible. The lack of an absorption feature at the GeV band confirms that the emission region of 3C 66A should be out of the inner zone of the BLR.

4 DISCUSSION AND CONCLUSIONS

A pure SSC model fails to explain the average GeV spectrum of 3C 66A observed by *Fermi*-LAT during its first three months of operation. However, a satisfactory reproduction of the data can be obtained by the multi-component model (see Figs. 2 and 3), which takes into account not only the specific shell structure of the BLR, but also the angular dependence of the photon distribution. The multi-component model requires a large value of $\gamma'_{\rm min} \sim 2 \times 10^3$. As argued by Tavecchio et al. (2009), this result seems to provide important clues about the electron acceleration process and the role of energy loss. A large value of $\gamma'_{\rm min}$ leads to a steep spectrum in the low-energy band, so our model does not explain the observed radio emission. The radio emission could come from a larger region that generates emission (e.g., Tang et al. 2010).

Based on the modeling results, we try to constrain the redshift of 3C 66A through connecting the GeV-TeV spectra. Because we cannot give the error estimate by using this method, we think only the redshift range that we derived is significant. It is therefore suggested that the redshift of 3C 66A could be between 0.1 and 0.3, and the most likely one is ~ 0.2. Furthermore, we found the results are independent of the assumptions that we made about the BLR structure. By using a different emission model and GeV-TeV data, we obtained very similar results as those obtained by Abdo et al. (2011). However, it should be kept in mind that both our results and those of Abdo et al. (2011) depend on the EBL model. We also try to get clues to the gamma-ray emission location of 3C 66A. Combining the BLR absorption effect and the EC component required to reproduce the gamma-ray emission, our results indicate that the gamma-ray emission region of 3C 66A could be in the outer zone of the BLR or out of the BLR.

Acknowledgements We thank the referee for constructive comments. We thank L. Zhang and X. W. Cao for helpful comments on this paper and J. P. Yang for helpful discussion. This work is supported by the National Science Foundation of China (Grant Nos. 11063003 and 10963004) and the Yunnan Provincial Science Foundation (grant 2009CI040).

References

Abdo, A. A., Ackermann, M., Ajello, M., et al. 2010a, ApJ, 723, 1082
Abdo, A. A., Ackermann, M., Agudo, I., et al. 2010b, ApJ, 716, 30
Abdo, A. A., Ackermann, M., Ajello, M., et al. 2011, ApJ, 726, 43
Acciari, V. A., Aliu, E., Arlen, T., et al. 2009, ApJ, 693, L104
Acciari, V. A., Aliu, E., Arlen, T., et al. 2010, ApJ, 721, L203
Aharonian, F., Akhperjanian, A. G., Bazer-Bachi, A. R., et al. 2006, Nature, 440, 1018
Albert, J., Aliu, E., MAGIC Collaboration, et al. 2008, Science, 320, 1752
Bai, J. M., Liu, H. T., & Ma, L. 2009, ApJ, 699, 2002
Bentz, M. C., Peterson, B. M., Netzer, H., Pogge, R. W., & Vestergaard, M. 2009, ApJ, 697, 160
Böttcher, M. 2007, Ap&SS, 309, 95
Böttcher, M., Fultz, K., Aller, H. D., et al. 2009, ApJ, 694, 174

Bramel, D. A., Carson, J., Covault, C. E., et al. 2005, ApJ, 629, 108
Dermer, C. D., & Schlickeiser, R. 1993, ApJ, 416, 458
Dermer, C. D., Finke, J. D., Krug, H., & Böttcher, M. 2009, ApJ, 692, 32
Donea, A.-C., & Protheroe, R. J. 2003, Astroparticle Physics, 18, 377
Finke, J. D., Shields, J. C., Böttcher, M., & Basu, S. 2008, A&A, 477, 513
Finke, J. D., Razzaque, S., & Dermer, C. D. 2010, ApJ, 712, 238
Finke, J. D., & Dermer, C. D. 2010, ApJ, 714, L303
Fiorucci, M., Ciprini, S., & Tosti, G. 2004, A&A, 419, 25
Franceschini, A., Rodighiero, G., & Vaccari, M. 2008, A&A, 487, 837
Gao, X.-Y., Wang, J.-C., & Zhou, M. 2011, RAA (Research in Astronomy and Astrophysics), 11, 902
Ghisellini, G., & Tavecchio, F. 2009, MNRAS, 397, 985
Ghisellini, G., Tavecchio, F., Foschini, L., et al. 2010, MNRAS, 402, 497
Joshi, M., & Böttcher, M. 2007, ApJ, 662, 884
Kaspi, S., & Netzer, H. 1999, ApJ, 524, 71
Kneiske, T. M., & Dole, H. 2010, A&A, 515, A19
Lanzetta, K. M., Turnshek, D. A., & Sandoval, J. 1993, ApJS, 84, 109
Liu, H. T., Bai, J. M., & Ma, L. 2008, ApJ, 688, 148
Mannheim, K. 1993, A&A, 269, 67
Maraschi, L., Ghisellini, G., & Celotti, A. 1992, ApJ, 397, L5
Miller, J. S., French, H. B., & Hawley, S. A. 1978, in Pittsburgh Conference on BL Lac Objects, ed. A. M. Wolfe (Pittsburgh, PA: Univ. Pittsburgh), 176
Mücke, A., Protheroe, R. J., Engel, R., Rachen, J. P., & Stanev, T. 2003, Astroparticle Physics, 18, 593
Perri, M., Massaro, E., Giommi, P., et al. 2003, A&A, 407, 453
Peterson, B. M., Berlind, P., Bertram, R., et al. 1994, ApJ, 425, 622
Poutanen, J., & Stern, B. 2010, ApJ, 717, L118
Prandini, E., Bonnoli, G., Maraschi, L., Mariotti, M., & Tavecchio, F. 2010, MNRAS, 405, L76
Razzaque, S., Dermer, C. D., & Finke, J. D. 2009, ApJ, 697, 483
Rees, M. J. 1967, MNRAS, 137, 429
Reimer, A. 2007, ApJ, 665, 1023
Shakura, N. I., & Sunyaev, R. A. 1973, A&A, 24, 337
Sikora, M., Begelman, M. C., & Rees, M. J. 1994, ApJ, 421, 153
Stecker, F. W., de Jager, O. C., & Salamon, M. H. 1992, ApJ, 390, L49
Stecker, F. W., Malkan, M. A., & Scully, S. T. 2006, ApJ, 648, 774
Stecker, F. W., & Scully, S. T. 2009, ApJ, 691, L91
Takalo, L. O., Sillanpaeae, A., Pursimo, T., et al. 1996, A&AS, 120, 313
Tang, Y.-Y., Dai, Z.-C., & Zhang, L. 2010, RAA (Research in Astronomy and Astrophysics), 10, 415
Tavecchio, F., Ghisellini, G., Ghirlanda, G., Costamante, L., & Franceschini, A. 2009, MNRAS, 399, L59
Véron-Cetty, M.-P., & Véron, P. 2010, A&A, 518, A10
Yan, D., Zeng, H., & Zhang, L. 2012, PASJ, 64, 80
Yang, J., & Wang, J. 2010, A&A, 511, A11